We are IntechOpen,
the world's leading publisher of
Open Access books
Built by scientists, for scientists

4,800
Open access books available

122,000
International authors and editors

135M
Downloads

154
Countries delivered to

Our authors are among the

TOP 1%
most cited scientists

12.2%
Contributors from top 500 universities

CLARIVATE ANALYTICS
BOOK CITATION INDEX
INDEXED

WEB OF SCIENCE™

Selection of our books indexed in the Book Citation Index
in Web of Science™ Core Collection (BKCI)

Interested in publishing with us?
Contact book.department@intechopen.com

Numbers displayed above are based on latest data collected.
For more information visit www.intechopen.com

Droplet-Based Microfluidic Scheme for Complex Chemical Reactions

Venkatachalam Chokkalingam[1], Ralf Seemann[2,3],
Boris Weidenhof[3] and Wilhelm F. Maier[3]
[1]Experimental Physics, Saarland University, Saarbrücken
[2]Max Planck Institute for Dynamics and Self-Organisation (MPIDS), Göttingen
[3]Technical Chemistry, Saarland University, Saarbrücken
Germany

1. Introduction

Liquid flow in microfluidic channels typically occurs at low Reynolds numbers, such that the flow is purely laminar [Solomon et al. 2003; Oddy et al. 2001]. As a consequence, two or more streams of miscible fluids flowing side-by-side only mix by diffusion. Such a mixing is very slow and it would be difficult to perform chemical reactions within the typical length scales respectively time scales used in standard microfluidic settings [Bruus et al. 2007; Stone et el., 2004; Teh et al., 2008]. Furthermore, the axial dispersion of concentration gradients parallel to the flow direction (Taylor dispersion [Taylor, 1954]) is a problem associated with the laminar flow in confined geometries due to the parabolic flow profile within microfluidic channels.

To overcome these microfluidic obstacles in mixing and to avoid axial dispersion, there has been considerable development towards the use of multiphase flows within microchannels. Continuous phase liquids can e.g. be segmented into allotments by injecting bubbles or droplets of a second immiscible fluid phase [Günther et al. 2004; Khan et al., 2004]. In this case, axial dispersion is eliminated because each liquid allotment is restricted between two bubbles and fast mixing is achieved by a friction induced circulating flow inside each allotment [Song et al., 2003 ; Li et al., 2007]. But as the liquid of each allotment is directly in contact with the microfluidic channel walls, cross-contaminations cannot be fully avoided and sticking of samples or reagents to the microchannel walls is unavoidable in this type of segmented flow microfluidics provided certain chemicals are processed.

Alternatively to the segmentation of a continuous flow by bubbles, reagents can be compartmented in emulsion droplets in a surrounding carrier phase for microfluidic processing. The latter approach is termed "droplet-based" microfluidic systems [Atencia & Beebe, 2005; Tabling, 2006]. The (emulsion-) droplets never get in contact with the channel walls and the sticking of reagents which are contained inside the droplets to the microfluidic channel walls is avoided. Mixing of a droplet content is also fast due to the friction induced convective flow pattern emerging inside droplets similar to the flow pattern in the

individual allotments of segmented flow microfluidics [Song et al., 2003 ; Li et al., 2007]. But even that the transport and the processing of liquids in the form of individual droplets has many benefits, the development of new techniques and approaches were required to make droplet based microfluidics a useful tool to perform complex chemical reactions.

The first crucial step is to dispense different reagents into individual droplets with good volume control. In initial approaches using droplets as micro-reactors, the different reactants were commonly dispensed into droplets from a single inlet channel [Song et al., 2003; Chen et al., 2005; Li et al., 2007]. Using this method, the reactants are already partly mixed and reactive at the channel inlet even before being dispersed into droplets. This method of common dispensing will thus result in channel clogging for fast chemical reactions where a gel or a precipitate is formed within milliseconds of contact.

The problem of channel clogging can be avoided by initiating the reaction inside droplets by either adding a reagent from a nozzle directly into passing droplets [Abate et al., 2010**]** or by combining two individual droplets containing the different reactants. The microfluidic reaction scheme of combining droplets on demand is feasible to process also reactive fluids, which might precipitate, solidify or stick to channel walls [Evans et al., 2009] and which cannot be processed in single phase microfluidics approaches. This reaction scheme enables a microfluidic device to function for a long operation time with stable reaction conditions. To perform droplet based chemical reactions in the above mentioned manner several issues have to be addressed: First, the volume of the chemicals needs to be known precisely for full control over the chemical reaction. Thus, primary droplet sizes have to be produced with excellent monodispersity. Second, at least two kinds of the primary droplets containing the different reactants have to be generated in a pair like manner. Thus either two trains of droplets have to be synchronized subsequent to droplet production or the droplet production has to be synchronized directly to form strictly alternating pairs of droplets containing the different chemicals. Third, we have to reliably combine the formed primary droplet pairs and mix the content of the subsequently formed secondary droplets to induce the desired chemical reaction. And last, we either have to observe and analyze the results *in-situ* in the microfluidic device or we have to collect and post-process the reactants outside of the microfluidic device.

In this chapter, we discuss a droplet-based microfluidic scheme to perform fast chemical reactions without channel clogging and with precise volume and process control. This microfluidic scheme enables a process to function for long operation times with stable conditions. For that every microfluidic processing step is considered and adapted to meet the experimental requirements. We discuss this scheme explicitly for the production of mesoporous silica particles and platinum doped silica particles from a sol-gel synthesis route for heterogeneous catalysis. In the first sections the emulsion system is introduced, the device fabrication, and its operation is explained followed by the basics of sol-gel chemistry and how to evaluate the results. In the subsequent sections the individual microfluidic techniques and their optimization for the considered sol-gel reaction are explained. The explanation of the individual techniques is followed by a discussion of the entire microfluidic scheme which is used for the production of silica and Pt-doped silica microspheres from a sol-gel synthesis route and finalized by the physical and chemical analysis of the microfluidically produced microspheres.

2. Background, materials and experimental set-up

2.1 Emulsion systems

Water-in-oil (W/O) emulsions are good candidates for applications where aqueous phase chemical reactions are required as the two liquid phases are immiscible and the droplets can be stabilized easily and also their volume is maintained. If additional organic phases like methanol are contained in the aqueous phase particular oils, like perfluorinated oils, have to be chosen as carrier fluids where neither of the compounds of the droplet phase is soluble. Throughout this chapter the following emulsion systems is applied: A water-methanol mixture containing reagents are dispensed in perfluorodecalin (PFD) ($C_{10}F_{18}$, ABCR GmbH, Germany), as the continuous oil phase. The emulsion system is stabilized by the fluorinated surfactant molecules penta decaflouoro-1-octanol ($C_8H_3F_{15}O$, ABCR GmbH & Co. KG) which are added to the PFD phase. To approximate the amount of surfactant needed to stabilize the oil/aq. phase - interface, the interfacial tension of water/PFD and water-methanol/PFD (with the vol. ratio of 60/40 of methanol/water) was determined as function of the surfactant concentration using the pendant drop method (OCA 20, Data Physics GmbH, Germany), c.f. fig. 1.
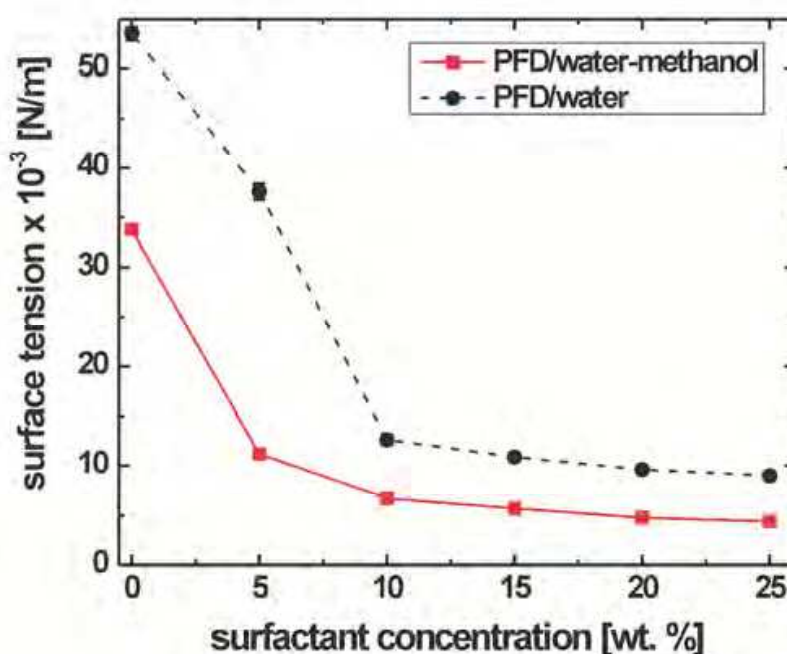

Fig. 1. Surface tension of perfluorodecalin/water and perfluorodecalin/methanol-water (60/40 v/v) interfaces as function of penta decaflouoro-1-octanol concentration.

I turns out that a surprisingly large amount of penta decaflouoro-1-octanol is needed to lower the interfacial tension to its plateau value. The addition of methanol (60 vol%) lowers the surface tension compared to pure water and increases the stability of the emulsion droplets significantly whereas the critical surfactant concentration needed to reach the plateau value is hardly affected by the addition of methanol. For the experiments discussed in this chapter 20 wt.% of penta decaflouoro-1-octanol is added to perfluorodecalin to lower the oil/water surface tension sufficiently to guarantee for stable droplet generation. However, penta decaflouoro-1-octanol stabilizes the droplets only weakly compared to

standard emulsion systems and allows for easy droplet coalescence techniques, as will be discussed later.

2.2 Microfluidic device fabrication

The fabrication of microfluidic devices has become one of the specialities of micro-electro-mechanical systems (MEMS). Silicon microfabrication was well-established already in integrated circuit (IC) processes and therefore first microfluidic systems applied silicon as a device material. On the other hand glass has been the traditional material for chemical vessels for analysis and reactions and was also a natural choice for first microchips. However, microfabrication in glass and silicon substrates is technical demanding due to several required fabrication steps like etching and wafer bonding. To accelerate device fabrication times and to increase fabrication volumes the typically much easier to handle polymer microfabrication techniques made their way. Today a wide selection of polymeric materials and fabrication techniques provide suitable materials and methods for most applications. For droplet-based microfluidics it is particularly important that the used device material has a suitable chemical resistance to the used organic carrier phase to avoid or minimize swelling and dissolution of the polymeric materials and to avoid diffusion of the organic carrier phase through the device material. Additionally, the wettability of the device material is very important in droplet based microfluidics as the carrier phase must preferentially wet the channel material to guarantee stable droplet generation.

The microfluidic devices used in this study are made of a commercially available Poly(dimethylsiloxane) (PDMS) elastomer kit, 'Sylgard 184' (SG184, Dow Corning), and were fabricated by soft lithographic techniques [Xia & Whitesides, 1998; Wong & Ho, 2009]. PDMS has a unique combination of properties resulting from the presence of an inorganic siloxane backbone and organic methyl groups attached to silicon. They have very low glass transition temperatures and are liquid at room temperature. These liquid materials can be readily converted into solid elastomers by a cross-linking reaction. A photo-lithographically prepared SU-8 structure on a silicon wafer was used as a mould with inverted pattern structure. The main steps of the device fabrication are sketched in fig. 2a.

The Sylgard 184 base and curing agent were mixed in a ratio of 10:1 w/w, degassed and decanted onto the SU-8 mould. Once mixed, poured over the master and heated to elevated temperatures, the liquid mixture becomes a cross-linked elastomer within a few hours via the hydrosilylation reaction between vinyl ($SiCH=CH_2$) groups and hydrosilane (SiH) groups [Whitesides et al., 2001]. The multiple reaction sites on both the base and crosslinking oligomers allow for three-dimensional crosslinking. After thermal curing overnight at 65 °C, the Sylgard 184 facilitates easy peeling of the cross linked silicon elastomer structure from the SU-8 mold. In order to use these structures as microfluidic device, inlet holes were punched and the channels were sealed by a glass cover. To bond the glass cover covalently to the PDMS device the PDMS surface was activated by an oxygen plasma (Diener electronic GmbH, Germany) [Whitesides et al., 2001; Eddings et al., 2008] rendering the PDMS surface hydrophilic. To finally produce stable aqueous drops in the surrounding perfluorinated oil phase within the PDMS microchannels, the surfaces of the bonded devices were rendered back to hydrophobic nature by heating the devices to 60 °C for at least 6 hours. Teflon tubing was connected to the punched holes (fig. 2b) and the other ends of the tubing were connected to glass syringes.
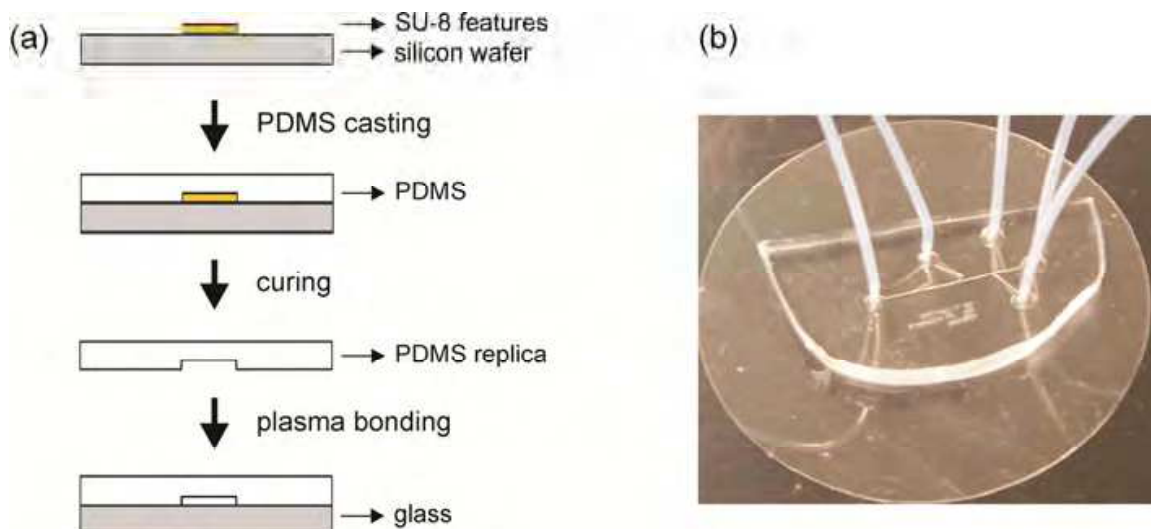
Fig. 2. (a) Schematic of PDMS Device Fabrication. (b) Ready to use PDMS device with tubes connected; the diameter of the cover glass slide: 5 cm.

2.3 Experimental set-up

A Leica Z16 APO optical microscope with a Leica L5 FL light source (fig. 3a), was typically used to monitor the microfluidic processes. Images and movies were recorded using a high resolution CCD camera (PCO 1600 hs, PCO AG, Germany); whenever needed, a high speed CMOS camera (PCO 1200 hs, PCO AG, Germany) was used which is able to capture more than 600 frames per second. Typical exposure times ranged from 500 µs to 50 ms, depending on flow velocity. The flow rates were adjusted precisely using custom-made syringe pumps (fig. 3b) driven by dc motors with decoder which were computer controlled using LabView programs (National Instruments Corporation). Using 1 ml gas tight precision glass syringes (Hamilton Bonaduz AG, Switzerland) volumetric flow rates between 10 µl/h and 1 ml/h were typically applied. Image analysis was done using the software: Image-Pro Plus 6.3 (Media Cybernetics, Inc., USA) and ImageJ 1.42 (National Institute for Health, USA).
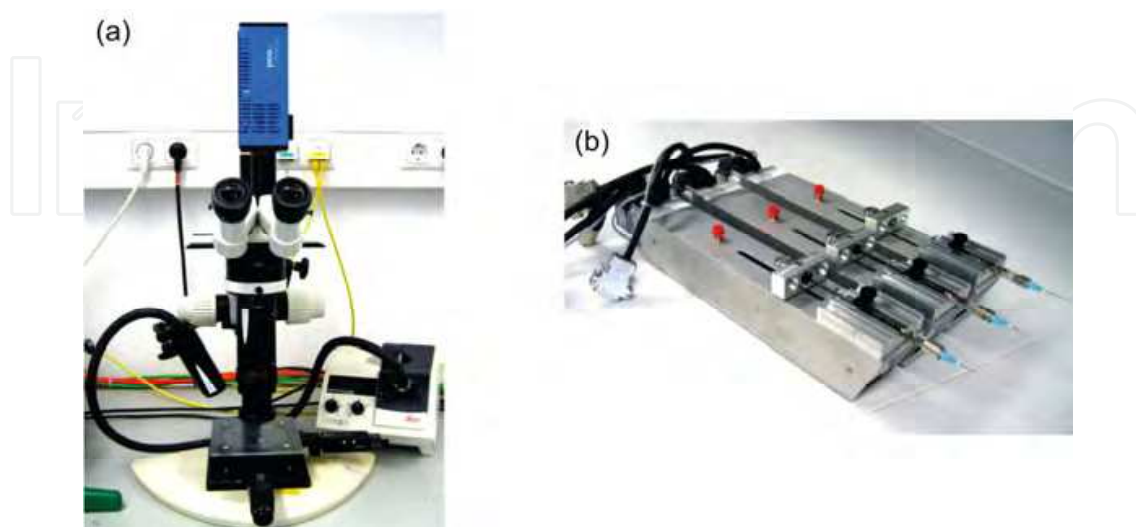

Fig. 3. a) Leica macroscope Z16 APO with a Leica L5 FL light source and camera. b) Custom made syringe pumps with glass syringes (Hamilton).

2.4 Sol-gel chemistry

Mesoporous materials with pores of 2 – 50 nm possess a potential combination of high surface areas and accessible pore sizes that make them ideal candidates for e.g. catalysts, catalyst supports and for the separation of complex molecules. A widely used material with such merits is mesoporous silica which is primarily produced through sol-gel processing. As we employ such a sol-gel process in our microfluidic approach, the reaction scheme will be explained in the following.
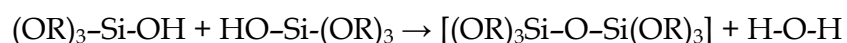
The most common starting point of the sol-gel process is the mixing of alkoxides (any organic compound derived from an alcohol by replacement of a hydrogen atom with a metal or other species) in a hydrolyzing environment (a chemical reaction of a compound with water). Gelation of the alkoxide solution occurs via a two-step process. First, alkoxides react readily with water. This reaction is called hydrolysis, because a hydroxyl ion becomes attached to the silicon atom as follows:
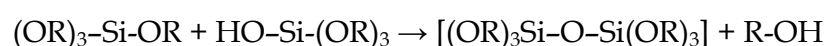
$$Si(OR)_4 + H_2O \rightarrow HO\text{-}Si(OR)_3 + R\text{-}OH$$

where R typically represents CH_3, C_2H_5, or C_3H_7. Depending on the amount of water and catalyst present, hydrolysis may proceed completely, so that all of the OR groups are replaced by OH groups, as follows:

$$Si(OR)_4 + 4\,H_2O \rightarrow Si(OH)_4 + 4\,R\text{-}OH$$
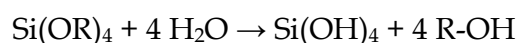
Any intermediate species $[(OR)_2\text{-}Si\text{-}(OH)_2]$ or $[(OR)_3\text{-}Si\text{-}(OH)]$ would be considered the result of partial hydrolysis. Two partially hydrolyzed molecules can link together in a condensation reaction to form a siloxane [Si–O–Si] bond:

$$(OR)_3\text{-}Si\text{-}OH + HO\text{-}Si\text{-}(OR)_3 \rightarrow [(OR)_3Si\text{-}O\text{-}Si(OR)_3] + H\text{-}O\text{-}H$$

or

$$(OR)_3\text{-}Si\text{-}OR + HO\text{-}Si\text{-}(OR)_3 \rightarrow [(OR)_3Si\text{-}O\text{-}Si(OR)_3] + R\text{-}OH$$

The condensation reaction liberates small molecule such as water or alcohol. These reactions can continue to build larger and larger silicon-containing molecules. The hydrolysis of the alkoxide can be catalyzed by both acids and bases, but the condensation step occurs much slower under acidic conditions. The hydrolysis and polycondensation reactions initiate at various sites within the precursor and the water as mixing occurs. When sufficient interconnected Si-O-Si bonds are formed in a region, they respond cooperatively as colloidal (submicrometer) particles or a sol. The size of the sol particles and the cross-linking within the particles depend upon the pH and the molar ratio r ($r = [H_2O]/[Si(OR)_4]$) [Brinker & Scherer, 1990]. As a function of time, the colloidal particles and the condensed silica species link together to a three-dimensional network.

The physical characteristics of the gel network depend largely upon the size of the formed particles and the degree of cross-linking prior to gel formation. At gel formation, the viscosity increases sharply and results in a gel. The gel is allowed to condense further during the following aging step (also called syneresis, which involves maintaining the gel for a period of time; hours to days) in order to increase the degree of cross-linking in the metal oxide network, and thereby to increase the strength and the structural stability of the

gel. After aging, the gel still contains excess water not used in hydrolysis of the alkoxide, alcohol produced during hydrolysis, and other additives present in the starting mixture. Accordingly, the gel must be dried under atmospheric conditions to remove these solvents. After drying, gels are calcined at a temperature of 550 °C in order remove the left-over organics and surface absorbed species. After this processing, the physical properties like surface morphology, pore size, and pore volume of the synthesized silica can be analyzed using the techniques which will be explained in the following sections.

The specific surface area and the pore structure of silica synthesized under strong acidic (pH < 2) or strong basic (pH > 12) conditions usually lead to silica with specific surface areas below 600 m²/g. Silica prepared under acidic conditions is microporous and has a fairly high surface area whereas the silica obtained under strong basic conditions (Stöber conditions [Stöber et al., 1968]) has a low surface area and is nonporous (pseudo mesoporous) [Tilgner et al., 1995]. To achieve a mesoporous silica with high surface area we will adopt a base catalyzed condensation at pH between 6 and 7 in our microfluidic scheme.

2.5 Techniques to evaluate the produced particles

In this section, the experimental techniques are shortly introduced which were used to quantify the properties of the produced silica (particles) with respect to physical and chemical properties like pore structure and composition.

Thermo-Gravimetric Analysis (TGA)

In our microfluidic approach silica gel particles were produced by means of droplet based microfluidics and collected outside of the microfluidic device. These silica gel particles have to be calcined to silica by a temperature treatment. To determine the ideal calcination temperature a thermo-gravimetric analysis (TGA) was performed using a TGA/DSC1 (Mettler-Toledo GmbH, Germany). The catalyst particles were filled into an alumina cup and heated at a ramp rate of 10 °C/min from ambient temperature to 800 °C. An empty alumina cup was used as the reference material. A flow of synthetic air (mixture of O_2 and N_2) of 40 ml/min, was maintained during the experiment. Evolving gases were monitored online with a Balzers ThermoStar GSD 300 T quadrupole mass spectrometer, see also fig. 9.

Specific surface area by physisorption

The porosity of the produced silica can be analyzed by 'physisorption'. The term 'physisorption' or 'physical adsorption' refers to the phenomenon of gas molecules adhering to a surface at a pressure less than their vapour pressure. The attraction between the adsorbed molecules and the surface are relatively weak. The energy of adsorption is approximately 20 kJ/mol, i.e. much lower than the typical strength of chemical bonds and therefore the adsorbed molecules retain their identities. An adsorption isotherm is recorded by carefully varying the partial pressure of the gas at constant temperature while the amount of the adsorbed gas is measured. The most widely used analysis of adsorption isotherms considers multilayer adsorption and was derived by Stephen **B**runauer, Paul **E**mmet and Edward **T**eller. Such a multilayer adsorption isotherm is called **BET** isotherm [Anderson et al., 1998; Brunauer et al., 2002]. Here, the initially adsorbed layer on a solid surface can act as a substrate for further adsorption and the adsorption isotherm is expected to rise infinitely, in contrast to a monolayer isotherm which saturates at high pressures (Langmuir isotherm [Langmuir, 1917]).

In our experiments, the specific surface area (m²/g) and pore volumes (cm³/g) of the porous silica was measured by the Brunauer-Emmet-Teller (BET) multipoint technique using an automated gas adsorption analyzer (Carlo Erba Sorptomatic 1990). The produced samples (at least 200 mg to achieve a good signal to noise ratio) were loaded and degassed at 200 °C for 2 h in vacuum, followed by the analysis of the surface area at the temperature of liquid nitrogen (77 K) with N_2 as adsorbate gas (the molecular area of the adsorbate N_2 is taken to be 15.8 Å²), see also Figs. 9 and 11.

Electron Microscopy and X-ray fluorescence

Hitachi S-4500 Scanning Electron Microscopy (SEM) was used in the presented work to image the surface structure of the produced catalyst particles with high magnification. For that, the catalyst particles were fixed to an electrically conducting carbon bed stuck to the SEM sample holder and then coated with thin gold layer to avoid charging effects. The accelerating voltage used for the measurements was 10 kV, see also figs. 10 and 12. To characterize the metal phase, JEOL JEM 2011 (JEOL GmbH, Germany) transmission electron microscopy (TEM) was used. An EDAX-Eagle II X-ray fluorescence (XRF) analyzer was used to analyze the platinum content in the microfluidically produced catalyst particles, see also fig. 14.

3. Microfluidic techniques

In this section the individual techniques will be explained in some detail, which are the basis of the microfluidic reaction scheme used in section 4 for the production of silica particles.

3.1 Synchronized droplet production

To perform chemical reactions by merging droplets inside a microfluidic device it is not just enough to produce one kind of monodisperse droplets. We rather have to produce two types of monodisperse droplets (with appropriate reagents) in a strictly alternating manner. Step emulsification geometry was demonstrated to produce droplets with excellent monodispersity (coefficient of variance in diameter < 1.2%) [Priest et al. (2006-1)]. The step geometry facilitates a triggered Rayleigh-Plateau type instability of a quasi 2d stream of an aqueous phase surrounded by an oily phase at a topographic step. For the synchronized production of two kinds of droplets having different chemical content, we combine two of these individual step-emulsification units into one double step-emulsification device (fig. 4A) [Chokkalingam et al., 2008]. A double-step-emulsification device consists of two single step-emulsification units combined to a common main channel, which is fed by the continuous oil phase.

A time series of the droplet formation process captured with the high speed camera is shown in fig. 4b: When a droplet is forming in one step-emulsification unit (e.g. bottom unit in fig. 4 b-a), the Laplace pressure of the forming drop decreases as its interface curvature decreases. This leads to a pressure drop redirecting the continuous phase flow towards this step-emulsification unit (bottom channel in Figure 4 b-b,c). During this droplet formation the volume flow of the continuous phase is hindered and the stream of dispersed phase coming from the upper step-emulsification unit retracts. When the dark droplet pinched-off into the main channel, the Laplace pressure changes rapidly, the stream of the dispersed

phase coming from the bottom unit retracts, and the continuous phase can flow more freely into the main channel (fig. 4 b-d). Subsequently, the dispersed phase coming from the top step-emulsification unit enters the main channel (fig. 4 b-e) and the process loops again. This pressure cross talk between the individual step-emulsification units synchronizes the drop production and leads to the defined formation of droplet pairs which might contain different reactants.
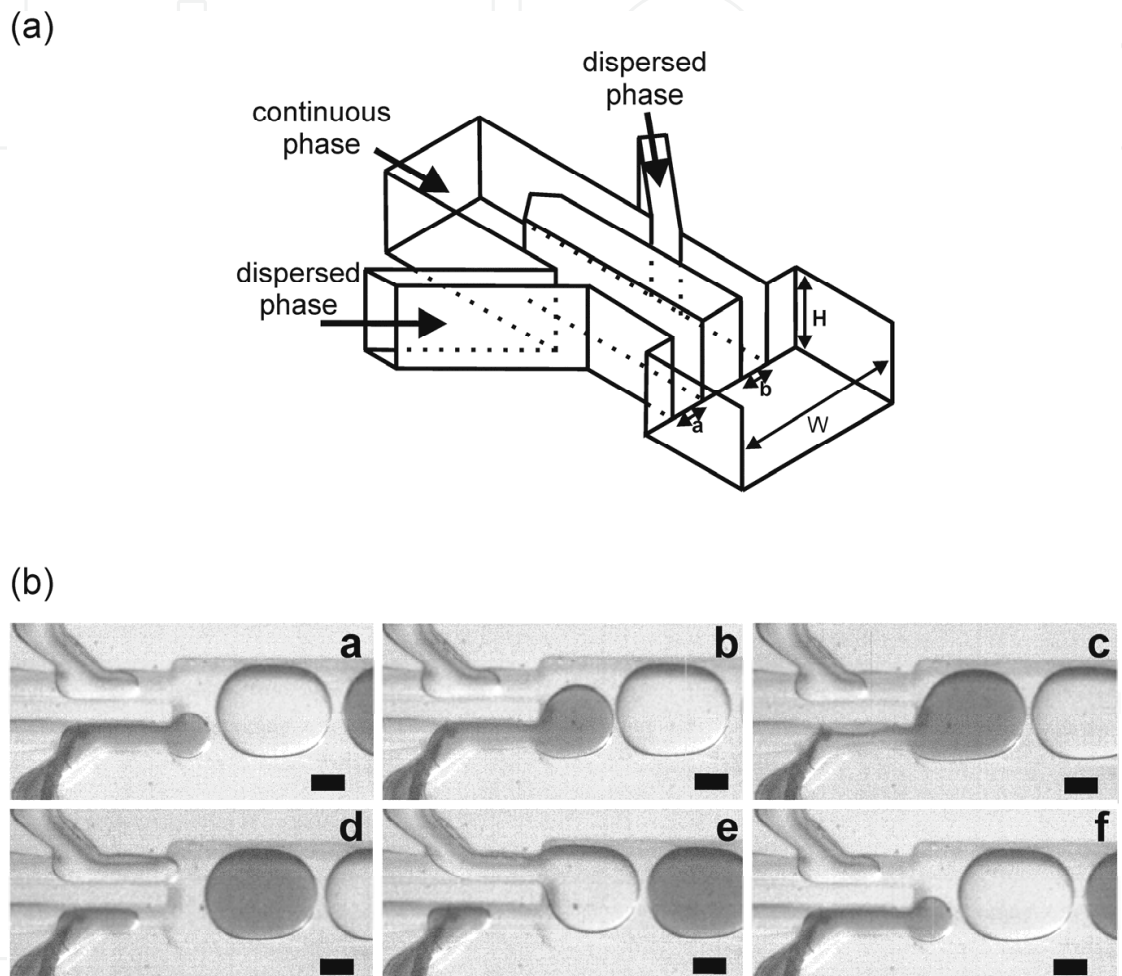
(a)

(b)

Fig. 4. (a) Schematic of the double step-emulsification device. The typical device dimensions were a = b = 35 µm, H = 120 µm and W = 160 µm. (b) Time series of optical images showing the droplet formation using a double step-emulsification device. For clarity, the aqueous phase injected from bottom is dyed with nile blue. Scale bar: 50 µm.

In case the volumetric flow rates of both step-emulsification units differ, the double step emulsification can produce droplet pairs having not only different chemical contents but also different volumes. In either case the volume control of each droplet type remains on the level of a single step emulsification device, i.e. having a variance in drop volume < 4%, see also fig. 5. For a better judgment of the dispersing precision for the reactants, we denote the droplet monodispersity in terms of droplet volumes rather than in droplet radius. The droplet volumes are calculated as follows: If the radius R of the projected droplet area is smaller or equal than the height of the microfluidic channel, the droplet is spherical and its volume can be simply calculated by $V = 4/3\ \pi R^3$. If the size of the droplets exceeds the

height of the channel h, as is our case, the droplets are assumed as disk shaped droplets and their volumes are calculated by $(\pi/12) \cdot [2D^3 - (D - h)^2 (2D + h)]$ where D is the diameter of the disk.
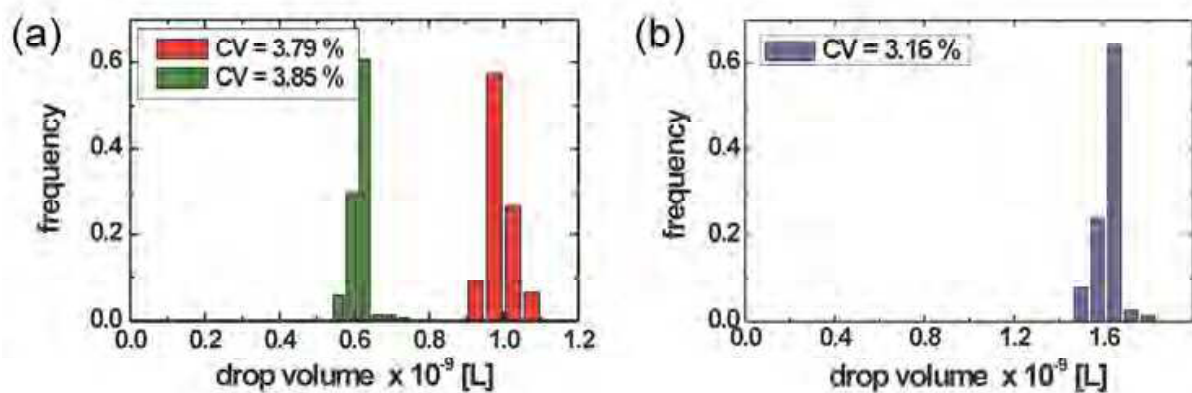

Fig. 5. (a) Histogram of the droplet volumes A and B that were generated with the self-synchronizing double step-emulsification device. (b) Histogram of the volumes of the merged droplets C.

The alternating droplet production is very robust, even up to about 300 droplets per second for the droplet size used here, and works up to a dispersed phase volume fraction of about 96 %. All these characteristics make the double step-emulsification device ideal for applications in complex microfluidic reactions.

3.2 Droplet merging and mixing

In the subsection before, it was explained how pairs of droplets can be produced in a strictly alternating manner. If the two droplets forming a pair contain different reactants, a chemical reaction can be initiated by merging and mixing the individual droplet pairs. In fig. 6, the controlled merging of two droplets, A and B, forming a pair and the subsequent droplet mixing in the combined droplet C is shown. The droplet merging can be achieved via a geometrical constriction as will be discussed in the following.

To keep the technical requirements for the drop coalescence as low as possible and still account for all experimental needs, we apply a technique where the aqueous droplet pairs are merged when they pass through a geometrical constriction. Such a merging technique works very effective for an emulsion system not being stabilized with surfactants or being stabilized with less effective surfactants, i.e. surfactants that do not stabilize the emulsion very well (c.f. section 2.1). When the droplet pairs reach a geometrical constriction, the merging of the two droplets is induced by slowing down the leading droplet at the constriction while the subsequently arriving droplet is pushed towards the first one (see fig. 6). If the constriction size is chosen appropriately, the droplets will pass the constriction during or right after the droplet coalescence. This technique has the lowest demands on the device fabrication and works very reliably also for droplet pairs arriving at the constriction with several hundred hertz. The precondition for the reliable droplet merging is that the droplet pairs arrive at the constriction with a certain separation from the previous and the

following droplet pairs. This can be achieved easily by producing two kinds of droplets having slightly different volumes: both kinds of droplets do not touch the side wall and experience the approximately parabolic flow profile in the microfluidic channel. Due to the parabolic flow profile, the smaller droplets move to the center of the channel where they experience a larger mean flow velocity and travel faster than the larger droplets. Accordingly, at a small distance downstream from the production unit, we find clearly separated droplet pairs where the larger droplet is leading and the smaller droplet is trailing behind (see fig. 6). The coalescence occurs at the constriction as explained earlier. Figure 5b shows the histogram of the volume of the merged gel drops *C*.
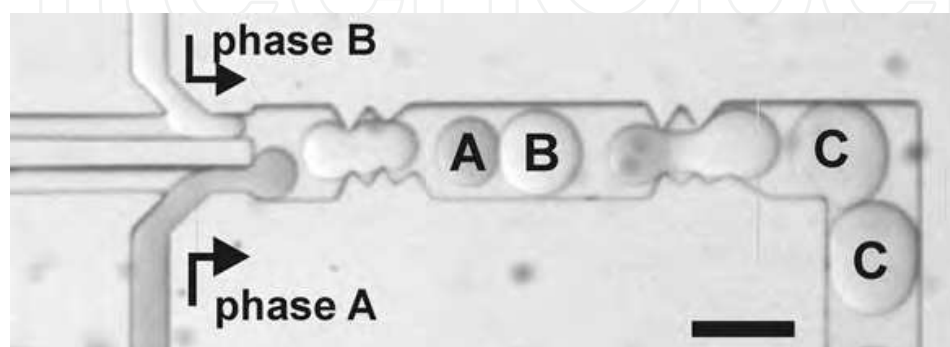
Fig. 6. Optical micrograph showing the production of droplets *A* and *B* having different volumes, the formation of separated droplet pairs lead by the bigger droplet and the subsequent coalescence into droplets *C* at a geometrical constriction. The aqueous phase injected from the bottom channel is colored with nile blue for clarity. Scale bar: 200 µm.

Downstream mixing of the reagents inside the combined droplet proceeds very efficiently due to the twisty flow pattern inside the droplets which is generated by the flow induced friction of the surfactant lamellae with the channel walls. Due to the dimensions typically used in microfluidic devices the circulating flow pattern emerging inside the travelling droplets is mirror symmetric with respect to a plane through the middle of the droplets parallel to the flow direction. Accordingly mixing occurs primarily within the 'top' and 'bottom' half of the droplet, whereas the mixing between the top and bottom half is slow which is a major obstacle if a chemical gradient is perpendicular to the flow direction. In this case the mixing can be accelerated by repeatedly altering the symmetry of the flow pattern using e.g. back fold channel geometries [Song et al, 2003]. However, in the situation considered here, where two droplets are combined that are flowing behind each other the resulting chemical gradient is parallel to the flow direction, c.f. the combined droplet in the constriction in Fig 6, and the symmetry of the concentration gradient does not need to be repeatedly varied to achieve fast mixing. With a concentration gradient parallel to the flow direction the elongation of the merged droplet at the constriction and the followed expansion in the wider channel additionally promotes fast mixing. In our experiments complete mixing is achieved within a travel distance of about 500 µm, i.e. about twice the droplet length, or about 100 ms at typical flow velocities of about 8 mm/s.

4. Microfluidic synthesis and analysis of silica particles

To produce silica particles by microfluidic routes, we optimized the individual microfluidic steps for this reaction, as explained in the previous section 3, and also optimized the sol-gel

recipe to adapt the gelation time to typical microfluidic processing time of a few seconds, cf. section 2. In this section we will now present the microfluidic reaction scheme for the fabrication of silica microspheres and discuss the achieved results.

The applied microfluidic sol-gel synthesis scheme is sketched in Scheme 1. One type of droplets, A, contains a 1.57 M acidified solution of the silica precursor tetramethoxysilane, TMOS ($Si(OCH_3)_4$, ABCR GmbH & Co. KG) in a mixture of methanol (Merck KGaA, Darmstadt, Germany) and water (Millipore™) at a volumetric ratio of 60/40 . The second type of droplets, B, contains ammonia (Merck KGaA, Darmstadt, Germany) based on the same water/methanol mixture. These two kinds of monodisperse droplets were produced with different volumes (fig. 5a) for the sake of the subsequent droplet merging as explained in section 3. A rapid acid catalyzed TMOS hydrolysis occurs in the aqueous solution A even before dispensing them into droplets at pH 1-2. Because of the high molar ratio of Si:H$_2$O ($r > 10$) and the nearly nonexistent retarding effect of the methoxide group on the hydrolysis rate, a rapid and nearly quantitative hydrolysis of the precursor to silicic acid can be assumed within a few minutes [Pouxviel et al., 1987]. The formation of the silica gel, however, is very slow at this pH. To accelerate the condensation of silicic acid in the microfluidic environment, we combined the TMOS containing droplets A with the ammonia containing droplets B to form droplets C and thereby adjust the pH to be between 6 and 7, above the iso-electric point of silica (pH > 3), where the gelation time is minimum [Stöber et al., 1968].
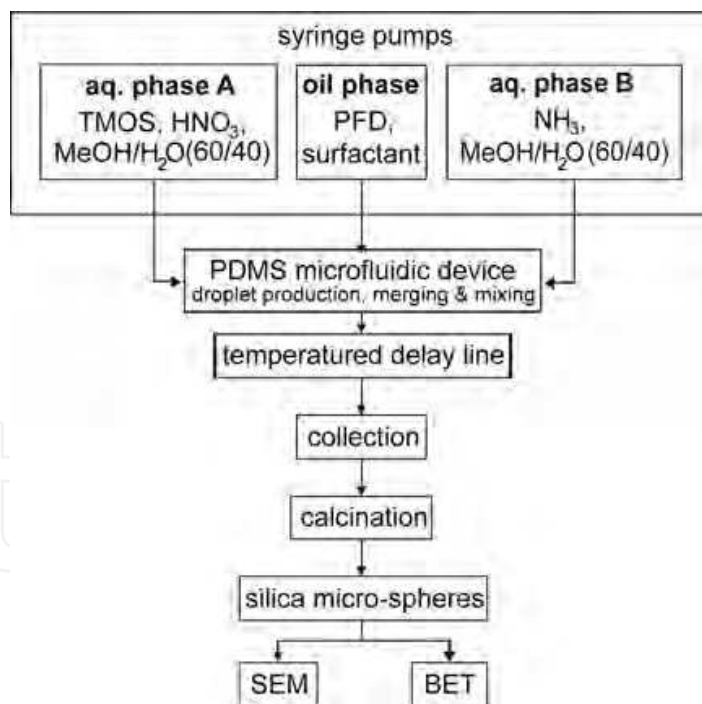
Scheme 1. Microfluidic synthesis route including the analysis of the produced silica spheres.

The final molar ratio in the mixed solution in droplet C was TMOS/methanol/HNO$_3$/NH$_3$/H$_2$O = 1/17.8/0.13/0.33/34.3. The condensation reaction starts with the deprotonation of silanols due to the reaction with hydroxyl ions. This condensation along with the aggregation of the condensed species leads to a continuous growth of the formed gel particles. This continues until the silica particles increasingly fuse and fill the complete drop

volume (drop volume determines particle size). Apart from the condensation, the dissolution of silica due to the reverse reactions of condensation also exhibits a strong pH-dependence which increases by more than three orders of magnitude between pH 3 and 8 in aqueous solution [Brinker & Scherer, 2000]. Due to the large methanol concentration in the merged droplet *C*, a low dissolution rate could be assumed as the solubility of silica in methanol is much lower than in water. During merging and mixing of droplets inside the microfluidic device, none of the reactive mixture gets in contact with the microfluidic channel which avoids any precipitation or sticking of the silica gel to the microfluidic channels and allows for long operation times.

Because of the large concentration of fluoroalkyl groups present in the surfactant being slightly soluble in the aqueous phase and the large surfactant concentration in the continuous phase, it seems possible that the pH of the aqueous solution is influenced. To guarantee that the pH of the merged droplets *C* is in the desired range for the sol-gel reaction, as adjusted by the reactant concentrations in droplets *A* and *B* we conducted two control experiments using the same microfluidic scheme: We added subsequently the pH indicators methyl red and bromothymol blue to one of the droplets [Methyl red: red at pH below 4.4, yellow at pH over 6.2, and orange in between (fig. 7a). Bromothymol blue: yellow at pH below 6, blue at pH over 7.6 and dark green in between (fig. 7b)]. With these reactions we could confirm that the pH inside the combined droplets *C* is in the range between 6.2 and 7.6 which is desired for fast gelation and we can exclude a significant pH change by the large concentration of surfactant.
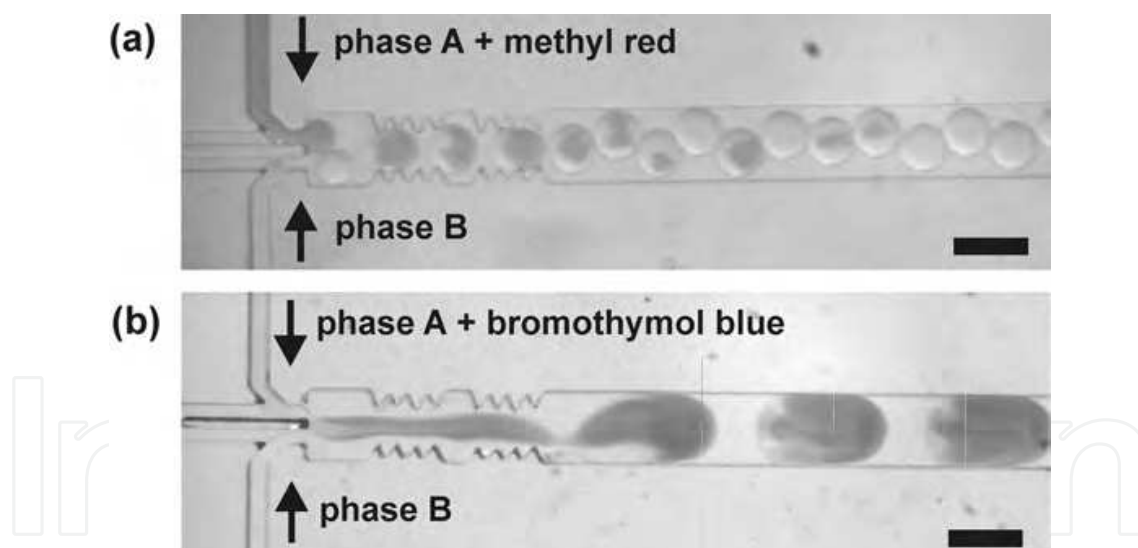

Fig. 7. Control experiments using pH sensitive dyes to determine the pH of the combined droplets *C*. (a) pH indicator: methyl red. The color change indicates a pH > 6.2. (b) pH indicator: bromothymol blue. The color change indicates a pH < 7.6. Scale bar: 150 μm.

To complete the microfluidic reaction scheme, the merged and mixed droplets *C* are subsequently given some time to develop the gel network. To avoid the formation of silica gel clumps at the rear side of the droplets [Evans et al., 2009], we guide the droplets into Teflon tubing with increased cross sectional area where the flow velocity is reduced by more than one order of magnitude. As the droplets do not touch the side walls of the Teflon tubing the convective flow pattern inside the droplets effectively vanishes. To guarantee that the gel

droplets stay separated in the Teflon tubing and do not start to clump together, the distance between them is slightly increased by adding a small percentage of continuous phase after the back fold channels (fig. 8), just before entering the Teflon tubing. The Teflon tubing is about 1 m in length and placed in a temperature controlled unit at 65 °C. The elevated temperature accelerates the gel formation and the removal of the solvent from the droplets.
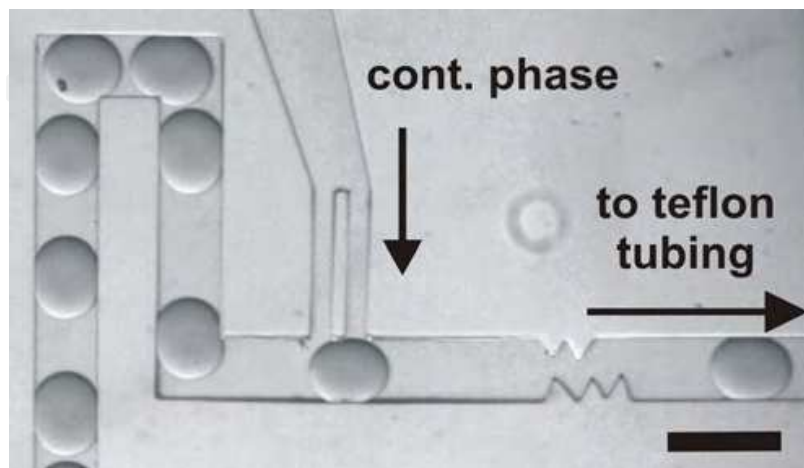

Fig. 8. Optical micrograph showing the end of the mixing line. The flow is from left to right. Right after the mixing line additional continuous oil phase is injected via the side channel to increasing the distance between the merged droplets before they enter the Teflon tubing. Scale bar: 200 μm.

The monodisperse silica particles are allowed to travel within the Teflon tube for about 20 min. Subsequently, they are collected outside of the microfluidic device in a beaker containing the same perfluorinated oil at the same temperature of 65 °C. In this beaker, the gel particles remain under continuous stirring for another 120 min, to ensure proper network formation and gentle solvent evaporation. The collected gel particles are removed from the beaker and subsequently stored at room temperature for about 48 hours. To remove the remaining organics and the surface absorbed species, the gel particles are calcined at elevated temperature. To identify the right temperature being sufficiently large to remove all organics and as low as possible not to densify the forming silica network, the evolving gases and the mass loss were monitored online as function of temperature, see fig. 9. With the help of the mass spectrometer signal, the mass loss of the samples can be divided into two main temperature regions: (1) between ambient temperature and 120 °C where water is evolved and (2) between 120 and 550 °C. Within the second region the feature between 120 °C to 250 °C denotes the temperature range where the PFD passes out whereas the plateau between 300 °C to 420 °C denotes the temperature range where PFD is combusted leading to CO_2 desorption. As a result, a minimum temperature of about 500 °C is required for calcination to expel all volatile organic components completely from the silica gel particles. Accordingly, all the collected gel particles that were used for the following analysis were calcined at a temperature of 550 °C.

The surface structure of the calcined silica particles are imaged by Scanning Electron Microscopy; images are displayed in fig. 10. The silica particles are almost perfectly round rarely showing small raised surface corrugations. The surface morphology is cloudy and reminiscent of a crumble topping.
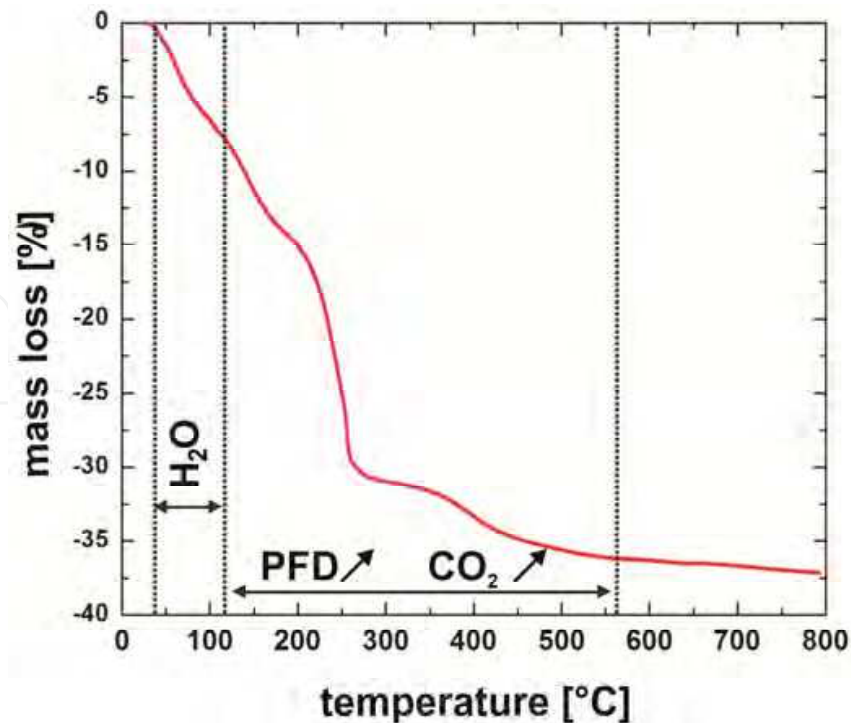
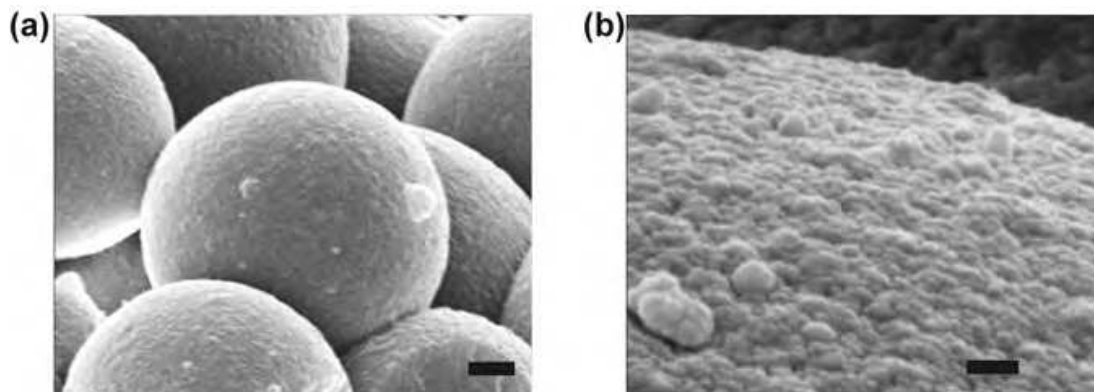Fig. 9. Thermo-Gravimetric Analysis curve of the produced silica particles.

Fig. 10. Scanning electron micrographs of silica spheres after calcinations. (a) Scale bar: 1 μm. (b) Close up of the surface structure. Scale bar: 50 nm.

The porosity and the pore volume of the produced silica particles were investigated by a BET analysis, c.f. section 2.5. A typical nitrogen adsorption-desorption isotherm recorded for the microfluidically synthesized silica particles is shown in fig. 11a. It shows a steep rise in the low-pressure region at a normalized pressure of about $p/p_0 < 0.05$ which indicates the presence of micropores in our analyzed silica samples. At larger partial pressure a characteristic hysteresis loop appears, between a relative pressure of $p/p_0 = 0.40$ and 0.85. According to IUPAC this type of isotherm can be classified as type IV and indicates the presence of mesopores (pore size 2 – 50 nm).Moreover, the shape of hysteresis indicates cylindrical pores with bimodal pore openings.. Based on the adsorption isotherm in fig. 11a the pore size distribution is calculated and displayed in fig. 11b. The pore size distribution (black solid curve in fig. 11b) is narrow having a distribution maximum at a pore radius of 2.4 nm.

The specific surface area of the produced silica particles averaged over several production runs and for various measurements was determined to 820 m^2/g (± 20 m^2/g) with a cumulative pore volume of 0.93 cm^3/g (± 0.02 cm^3/g).
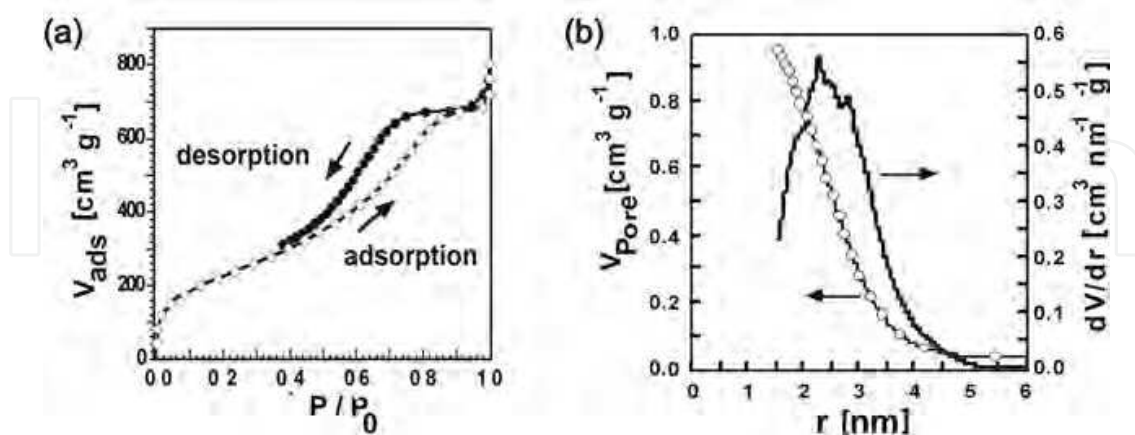

Fig. 11. (a) BET nitrogen adsorption-desorption isotherm of the produced silica spheres. V_{ads} = adsorbed volume, p/p_0 = reduced pressure (b) Pore size distribution. V_{pore} = pore volume, r = pore radius.

The specific surface area of the microfluidically produced silica spheres reveal significant differences compared to bulk synthesized silica using the same chemical recipe. For the microfluidically synthesized material we achieved a surface area which is about 40 % larger than the corresponding bulk value which is below 600 m^2/g. The surface area of the microspheres itself is just about 1 m^2/g and negligible with respect to the total surface area.

In order to further evaluate the superior results of our microfluidic reaction scheme, we compare the properties of our microfluidically produced silica particles to other microfluidic synthesis routes by Carroll *et al.* [Carroll et al., 2008], Lee *et al.* [Lee et al., 2008], Chen *et al.* [Chen et al., 2008]. However, the formation of mesoporous silica particles differ from our chemical scheme as the silica formation in these references was supported by surfactant templates as the solvents evaporate into the continuous carrier phase and cannot be compared directly. Furthermore, the microfluidically produced silica spheres in these references were not analyzed explicitly in terms of surface area and pore structure and rather results from bulk processing using the same chemical recipes were adopted. This might be a consequence of the limited operation time of the microfluidics device due to channel clogging and the presumably small amount of produced material which was not sufficient for a detailed analysis of the pore structure. Comparing our results to the adopted bulk results from Carroll et al., and Chen et al., we achieved a 50 % larger specific surface area even without surfactant templating due to the optimized droplet-based microfluidic reaction scheme.

5. Microfluidic synthesis of precious metal catalysts

Due to their enormous internal surface area and their homogeneous pore size distribution the microfluidically produced silica particles seem to be ideal supports for catalytically active elements. Platinum (Pt) or palladium (Pd) doped silica catalysts [Yazawa et el., 2002] are e.g. highly active for catalytic combustion of hydrocarbon and other organic exhausts.

Yao et al. [Yao et al., 1980] investigated the propane oxidation reactions and found Pt doped materials to be better catalysts than Palladium and Rhodium doped materials. In the following we modify the chemical recipe and use the above presented microfluidic reaction scheme to produce Pt doped silica spheres.

Platinum compounds ($Pt(NO_3)_2$) were readily dissolved in an aqueous phase and can thus be applied in a straight forward manner to the production of platinum doped silica spheres using the same microfluidic scheme as discussed above. Thus $Pt(NO_3)_2$ was added (up to about 7 mol.% (46 wt.%) of Pt) to the silica precursor tetramethoxysilane (TMOS) in a mixture of methanol and water at a volumetric ratio of 60/40 as dispersed phase *A*. The dispersed phase *B* contains again ammonia based on the same water/methanol mixture. Following the above described microfluidic protocol, platinum doped silica particles were produced, post-processed and analyis. The surface morphology of these particles depends on their Pt concentration as is evident from scanning electron micrographs. The SEM images displayed in fig. 12 reveal that the surface morphology of catalyst particles get rougher and cloudier as the Pt concentration increases.
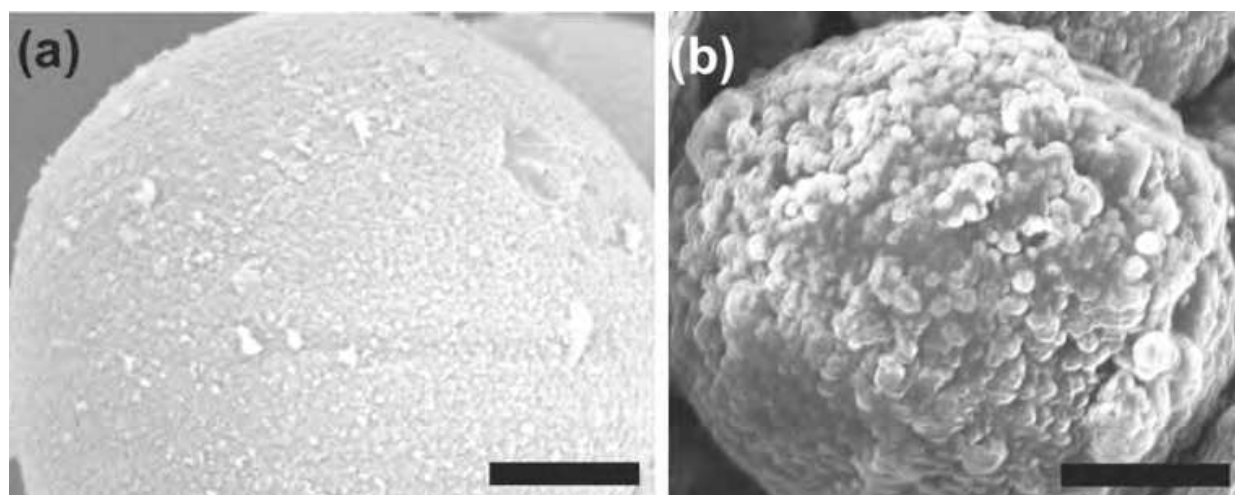

Fig. 12. SEM images of Pt doped silica particles: (a) 3 mol.%, (b) 7 mol.%. Scale bar: 1 μm.

We analyzed again the surface area and pore structure of the microfluidically synthesized platinum doped silica particles by a BET analysis. The specific surface area of the microfluidic catalyst particles with 4.91 mol.% platinum concentration averaged over several production runs and for various measurements was determined to be around 590 m²/g (± 20 m²/g) with a pore size distribution maximum at 1.9 nm (± 0.1 nm) pore radius and a cumulative pore volume of 0.54 cm³/g (± 0.02 cm³/g). Platinum concentration was also varied to 0.15 mol.% and the results are displayed in Table 1. The BET isotherm for 4.91 mol.% Pt concentration is shown in fig. 13.

Transmission electron micrographs indicate that the microfluidically produced silica particles contain metallic platinum (face centered cubic lattice) arranged in nanoscopic dots of about 2 nm size, see fig. 14. Based on the pore structure, the large surface area and the distribution of metallic platinum the microfluidically synthesized Pt doped silica particles are expected to be excellent catalysts for heterogeneous catalysis in general and for propane oxidation in particular.
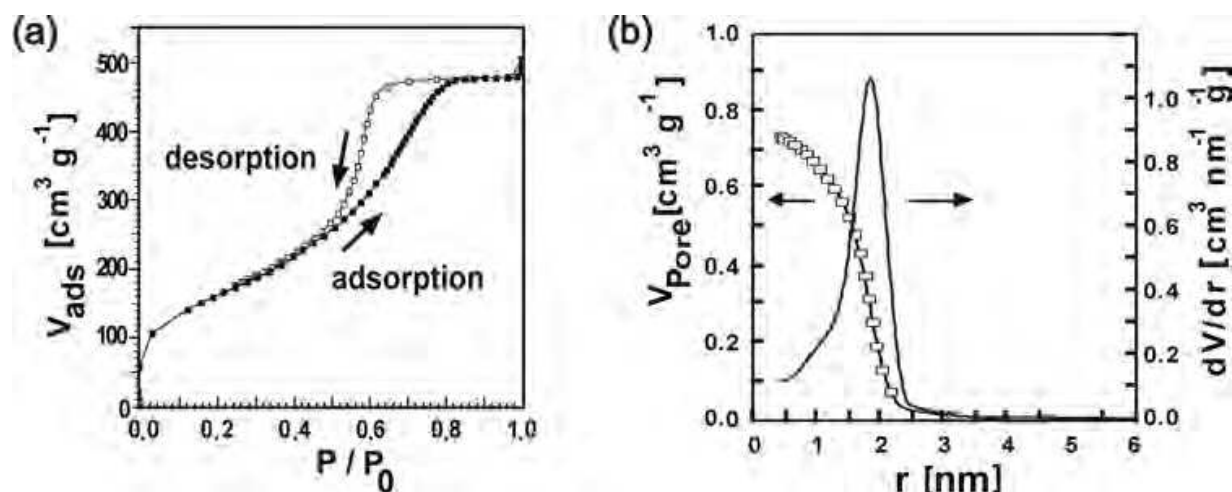
Fig. 13. BET nitrogen adsorption-desorption isotherm of the platinum doped silica catalyst microspheres produced through our microfluidic reaction scheme. V_{ads} = adsorbed volume, p/p_0 = reduced pressure.
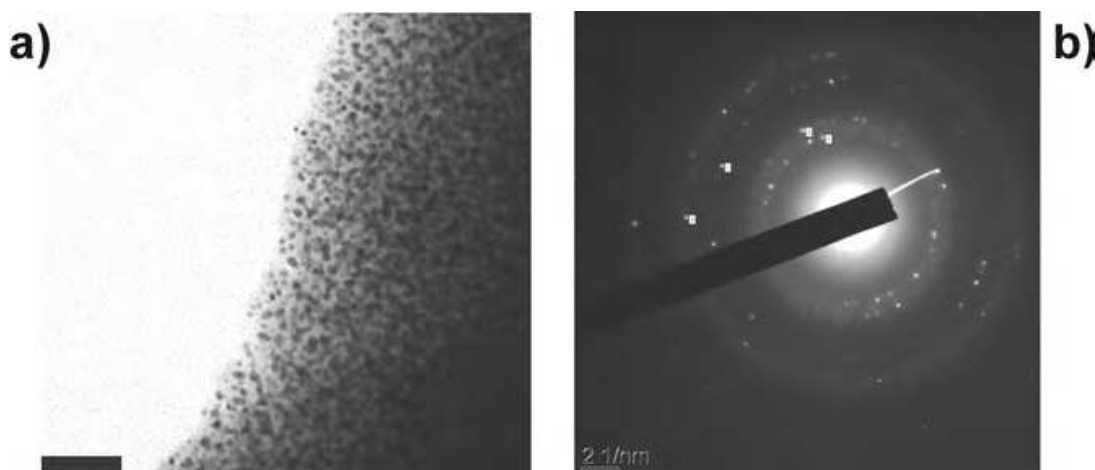

Fig. 14. TEM measurements of microfluidically synthesized platinum doped silica. a) TEM micrograph; scale bar: 100 nm.' b) electron diffraction pattern of the Pt nanodots. The face centered cubic lattice indicates metallic Pt; scale bar 2 nm^{-1}.

Material	Specific Surface Area (m²/g)	Pore radius (nm)	Cumulative pore volume (cm³/g)
SiO$_2$ particles	820 (± 20)	2.4	0.61 (± 0.02)
0.15 mol.% Pt/SiO$_2$ particles	592 (± 20)	1.961	0.58 (± 0.02)
4.91 mol.% Pt/SiO$_2$ particles	590 (± 20)	1.994	0.54 (± 0.02)

Table 1. Characterization results from the BET isotherms and XRF Analysis.

6. Conclusion

We discussed a droplet-based microfluidic reaction scheme to perform chemical reactions with precise volume and process control that allows for fast reactions that might even form gels or precipitates. The important step for the microfluidic scheme is the handling of the reactive

chemical mixture that never touches the channel walls and allows for long and stable operation conditions. We applied this microfluidic scheme to perform sol-gel reactions and produced silica particles and platinum doped silica particles with superior properties.

To achieve the synchronized production of droplet pairs containing different reactants a double step-emulsification device was used. Each kind of droplets containing the different reactants is produced with precise volume control and adjustable production frequency. The synchronization mechanism is very robust and makes the step-emulsification devices ideal for complex chemical reactions. The gel formation inside the droplets is started by a controlled merging of the droplet pairs at a geometric constriction forming droplets with a concentration gradient parallel to the flow direction. Mixing of the reactants inside the merged droplets is very fast due to the particular concentration gradient and a friction induced convective flow pattern. To optimize the protocol for the considered sol-gel reaction, an additional delay line and a thermal post processing line are included into the microfluidic device.

The silica particles produced by this microfluidic reaction scheme were mesoporous and had a superior surface area of 820 m²/g (± 20 m²/g) and a narrow pore radius distribution of around 2.4 nm. This surface area is about 40 % larger than the corresponding value of bulk synthesized silica using the same chemical recipe. The efficient mixing of reagents within the combined droplets and the short diffusion paths for the liquids in the droplets during the drying process help to achieve this improved quality. Without any modification in the microfluidic reaction scheme, the same protocol was further used to produce platinum doped silica catalyst particles by modifying the sol-gel recipe. The surface areas of the produced Pt doped particles are reduced to ~ 590 m²/g (± 20 m²/g) compared to pure silica spheres but still large compared to other synthesize schemes and are assumed to result in excellent catalytic activities.

From the obtained results we conclude that droplet-based microfluidic reaction schemes offer great possibilities to perform complex chemical reactions and to synthesize materials with superior properties which were not possible with existing microfluidic approaches. This type of droplet-based microfluidic scheme is thus expected to have a large potential not only for synthesis reactions but also for drug screening purposes or even combinatorial approaches when being combined with techniques to manipulate, redistribute and split merged droplets.

7. Acknowledgments

8. References

Abate A., Hung T., Mary P., Agresti J., and Weitz D. (2010), Proc. Natl. Acad. Sci., 107, 19163-19166.

Anderson K. T., Martin J. E., Odinek J. G., and Newcomer P. P., (1998) Chem. Mater. 10, 311-321.

Andersson N., Kronberg B., Corkery R., Alberius P. (2007), Langmuir, 23, 1459.

Atencia J. and Beebe D. J. (2005), Nature, 437, 648–655.

Barrett E. P., Joyner L. G., and Halenda P. P. (1951), Journal of the American Chemical Society, 73, 373-380.

Brinker C. J., Scherer G. W. (1990), Sol-Gel Science: The Physics and Chemistry of Sol-Gel Processing, Academic Press, Inc., Boston, ISBN: 0121349705.

Broekhoff J. C. P. and de Boer J. H. (1968), Journal of Catalysis, 10, 368-376.

Brunauer S., Emmett P. H. and Teller E. (2002), Journal of the American Chemical Society, 60, 309-319.

Bruus H. (2007), Theoretical Microfluidics, Oxford University Press, USA, ISBN 0199235090.

Carroll N. J., Rathod S. B., Derbins E., Mendez S., Weitz D. A. and Petsev D. N. (2008) Langmuir, 24, 658-661.

Chen D. L., Gerdts C. J., Ismagilov R. F. (2005) J. Am. Chem. Soc., 127, 9672.

Chen Y., Wang Y. J., Yang L. M. and Luo G. S. (2008), AIChE Journal, 54, 298-309.

Chokkalingam V., Herminghaus S. and Seemann R. (2008), Appl. Phys. Lett., 93, 254101-254103

Chokkalingam V., Weidenhof B., Krämer M., Herminghaus S., Seemann R., and Maier W. F. (2010), ChemPhysChem, 11, 2091 - 2095.

Eddings M., Johnson M., and Gale B. (2008), J. Micromech Microeng., 18, 067001.

Evans H., Surenjav E., Priest C., Herminghaus S., Seemann R. and Pfohl T. (2009), Lab Chip, 9, 1933-1941.

Günther A., Khan S. A., Thalmann M., Trachsel F., Jensen K. F. (2004), Lab on a Chip, 4, 278-283.

Langmuir I. (1917), J. Am. Chem. Soc., 39 (9), 1848-1906.

Lee I., Yoo Y., Cheng Z., Jeong H.-K. (2008), Adv. Funct. Mater., 18, 4014-4021.

Li L., Boedicker J. Q., Ismagilov R. F. (2007), Anal. Chem., 79, 2756.

Khan S. A., Günther A., Schmidt M. A. and Jensen K. F. (2004), Langmuir, 20, 8604–8611.

Oddy M. H., Santiago J. G., and Mikkelsen J. C. (2001), Anal. Chem. 73, 5822–5832.

Pouxviel J. C., Boilot J. P., Beloeil J. C. and Lallemand J. Y. (1987), Journal of Non-Crystalline Solids, , 89, 345-360.

Priest C., Herminghaus S., and Seemann R. (2006-1), Appl. Phys. Lett., 88, 024106.

Priest C., Herminghaus S., and Seemann R. (2006-2), Appl. Phys. Lett., 89, 134101

Solomon T. H., Mezic I. (2003) Uniform resonant chaotic mixing in fluid flows. Nature 425: 376–380.

Song H., Tice J. D. and R. F. Ismagilov (2003) Angew. Chem. Int. Edt., 42, 768-772.

Srinivasan V., Pamula V. K., and Fair R. B. (2004), Analytica Chimica Acta, 507, 145-150.

Stöber W., Fink A., Bohn E. (1968), J. Colloid Interf. Sci., 26, 62-69.

Stone H. A., Stroock A. D. and Ajdari A. (2004), Annual Review of Fluid Mechanics, 36, 381-411.

Storck S., Bretinger H., and Maier W. F. (1998), Applied Catalysis A: General, 174, 137-146.

Tabling P. (2006), Introduction to Microfluidics, Oxford University Press., ISBN: 0198568649.

Taylor G. (1954), Proceedings of the Royal Society of London, Series A. Mathematical and Physical Sciences, 225, 473-477.

Teh S.-Y., Lin R., Hung L.-H. and Lee A. P. (2008), Lab on a Chip, 8, 198-220.

Tilgner I. C., Fischer P., Bohnen F. M., Rehage H., Maier W. F. (1995), Microporous Mater., 5, 77-90.

Whitesides G. M., Ostuni E., Takayama S., Jiang X., and Ingber D. E. (2001), Annu. Rev. Biomed. Eng., 335–373.

Wong I. and Ho C.-M. (2009), Microfluidics and Nanofluidics, 7, 291.

Xia Y. and Whitesides G. M. (1998), Annu. Rev. Mater. Sci., 28,153–84.

Yazawa Y., Takagi N., Yoshida H., Komai S.I., Satsuma A., Tanaka T., Yoshida S., Hattori T., (2002) Appl. Catal. A 233, 103.

Yao Y. F. (1980), Ind. Eng. Chem . Prod. Res. Dev. 19, 293.
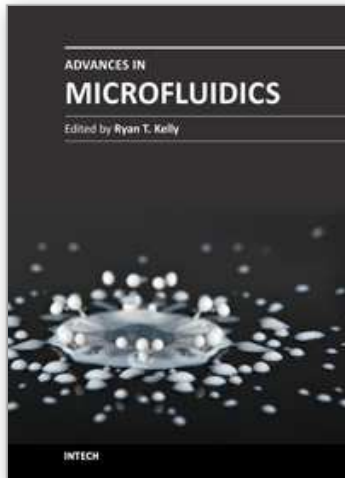
Advances in Microfluidics

Edited by Dr. Ryan Kelly

Advances in Microfluidics provides a current snapshot of the field of microfluidics as it relates to a variety of sub-disciplines. The chapters have been divided into three sections: Fluid Dynamics, Technology, and Applications, although a number of the chapters contain aspects that make them applicable to more than one section. It is hoped that this book will serve as a useful resource for recent entrants to the field as well as for established practitioners.

How to reference

In order to correctly reference this scholarly work, feel free to copy and paste the following:

Venkatachalam Chokkalingam, Ralf Seemann, Boris Weidenhof and Wilhelm F. Maier (2012). Droplet-Based Microfluidic Scheme for Complex Chemical Reactions, Advances in Microfluidics, Dr. Ryan Kelly (Ed.), ISBN: 978-953-51-0106-2, InTech, Available from: http://www.intechopen.com/books/advances-in-microfluidics/droplet-based-microfluidic-scheme-for-complex-chemical-reactions

INTECH
open science | open minds